

Estimating an Inverse Gamma distribution

A. Llera, C. F. Beckmann.

Technical report
Radboud University Nijmegen
Donders Institute for Brain Cognition and Behaviour.

Abstract

In this paper we introduce three different algorithms based on method of moments, maximum likelihood and full Bayesian estimation for learning the parameters of the Inverse Gamma distribution. We also provide an expression for the KL divergence for Inverse Gamma distributions which allows us to quantify the estimation accuracy of each of the algorithms. All the presented algorithms are novel. We consider most relevant the introduction of a conjugate prior for the Inverse Gamma shape parameter which enables the Bayesian inference procedure; in order to compute expectations under the proposed distribution we use the Laplace approximation. The introduction of this new prior allows analytical inference of the parameter estimation problem and also opens the possibility of including Inverse Gamma distributions into more complex Bayesian structures, e.g. mixture models. The algorithms introduced in this paper are computationally compared using synthetic data and interesting relationships between the maximum likelihood and the Bayesian approach are derived.

1 Introduction

The Inverse Gamma distribution belongs to the exponential family and has positive support. In most cases, the Gamma distribution is the one considered for modeling positive data [1, 13, 9, 7], and the Inverse Gamma remains marginally studied and used in practice. Although both distributions have similar properties, an important structural difference between them is that while the Inverse Gamma mode is always positive the Gamma one can be zero; this fact makes the Inverse Gamma very attractive to for example distinguish some kind of positive activation from stochastic noise usually modeled using a Gaussian distribution [2, 12]. The interesting qualities of the Inverse Gamma distribution as well as the absence of analytical expressions for the estimation of all its parameters motivates our search for efficient algorithms to estimate inverse gamma distributions.

The most traditional approach considered to estimate the parameters of a distribution is the Method of Moments (MM). This method can be attributed to Pearson [10] and it can be applied to any distribution for which there exists a unique relationship between its moments and parameters. In cases where the moments of a distribution can be mapped to the distributional parameters, the MM uses a Gaussian approximation to the moments to provide a closed form parameters estimation. The MM estimation is known to exist for the Gamma distribution, the Beta distribution or the Pareto distribution ¹. Another classic approach for parameter estimation is the well known

¹<http://www.math.uah.edu/stat/point/Moments.html>

maximum likelihood (ML), based in the maximization of the data log-likelihood; historically it is known to have been used by Gauss or Laplace amongst others [5] but it was after the 1950s with the appearance of modern computers that it became relevant in practice; Fisher is believed to have been the first one using ML in the computational field. While the MM and ML approaches provide point estimates for the distribution parameter values, a full Bayesian estimation approach introduces distributions over the parameters [8]; when choosing conjugate prior distributions over the parameters [8, 3], the posterior expectations can be analytically derived.

Surprisingly, as far as we know, the method of moments estimation for the Inverse Gamma is not present in the literature. Further, it is well known that one can find a ML solution for the Inverse Gamma scale parameter for a given shape parameter. However, it is not possible to find a ML closed form solution for the shape parameter and in practice numerical optimization is required [2, 12]. Regarding the Bayesian estimation, the conjugate prior for the scale parameter is known to be Gamma distributed [6] but there is no conjugate prior for the shape parameter present in the literature.

In section 2 we introduce all the methods considered in this article. In section 2.1 we introduce the Method of Moments, in section 2.2 a novel Maximum Likelihood algorithm and in section 2.3 we introduce the Bayesian parameter estimation strategy; section 2.3.1 reviews the methodology to find the scale posterior expectation and in section 2.3.2 we introduce a novel conjugate prior for the shape parameter that allows for the first time the analytic shape posterior estimation. To be able to asses the quality of each algorithm, in section 2.4 we introduce the KL-divergence between two Inverse Gamma distributions. Then, in section 3 we provide some theoretical comparison between the presented ML and Bayesian strategies as well as a numerical comparison between the three algorithms; in section 3.1 we provide examples demonstrating the ability of the new presented Bayesian strategy to correctly estimate the posterior shape value and in section 3.2 we compare the three presented algorithms. We conclude the paper with a brief discussion in section 4.

2 Methods

Consider the Inverse Gamma distribution

$$\mathcal{IG}(x|\alpha, \beta) = \frac{\beta^\alpha x^{-\alpha-1}}{\Gamma(\alpha)} \exp\left(\frac{-\beta}{x}\right), \quad (1)$$

defined for any positive real parameter values α and β , denoting the distribution shape and scale respectively, and where Γ is the Gamma function. The Inverse Gamma is defined over the support $x \in \mathbb{R}^+$ and its first two moments are [4]

$$\mathbb{E}_{\mathcal{IG}}[x] = \frac{\beta}{\alpha - 1} \quad \mathbb{E}_{\mathcal{IG}}[(x - \mathbb{E}_{\mathcal{IG}}[x])^2] = \frac{\beta^2}{(\alpha - 1)^2(\alpha - 2)}. \quad (2)$$

Given a vector of positive real values $\mathbf{x} = \{x_1, \dots, x_n\}$, in the following subsections we present different algorithms to find posterior estimations $\hat{\alpha}$ and $\hat{\beta}$ for the distribution parameters α and β .

2.1 Method of Moments (MM)

Using a Gaussian approximation to the moments of the Inverse Gamma distribution (2) we obtain the following:

$$\mu \approx \frac{\beta}{\alpha - 1}, \quad v \approx \frac{\beta^2}{(\alpha - 1)^2(\alpha - 2)},$$

where μ and v are the mean and variance estimated from the observed data vector $\mathbf{x} = \{x_1, \dots, x_n\}$. Solving this system for α and β we obtain

$$\hat{\alpha} \approx \frac{\mu^2}{v} + 2, \quad \hat{\beta} \approx \mu \left(\frac{\mu^2}{v} + 1 \right). \quad (3)$$

These closed form solutions form the basis of the MM estimation for the parameters of the Inverse Gamma distribution. Algorithm 1 summarises the process.

Algorithm 1 MM for Inverse Gamma

Require: $\mathbf{x} = \{x_1, \dots, x_n\}, x_i > 0$

$$\mu = \frac{1}{n} \sum_{i=1}^n x_i$$

$$v = \frac{1}{n-1} \sum_{i=1}^n (x_i - \mu)^2$$

$$\hat{\alpha} = \frac{\mu^2}{v} + 2$$

$$\hat{\beta} = \mu \left(\frac{\mu^2}{v} + 1 \right)$$

return $\hat{\alpha}, \hat{\beta}$

2.2 Maximum Likelihood (ML)

The log-likelihood of the positive vector of observations $\mathbf{x} = \{x_1, \dots, x_n\}$ under the Inverse Gamma distribution (1) can be written as

$$\log \mathcal{IG}(\mathbf{x}|\alpha, \beta) = -n(\alpha + 1) \overline{\log \mathbf{x}} - n \log \Gamma(\alpha) + n\alpha \log \beta - \sum_{i=1}^n \beta x_i^{-1} \quad (4)$$

where the upper bar operand indicates the arithmetic mean. Finding ML estimations for the parameters is achieved by maximizing equation (4) with respect to the parameters $\{\alpha, \beta\}$; it is easy to verify that equation (4) has a maximum at

$$\beta = \frac{n\alpha}{\sum_{i=1}^n x_i^{-1}}, \quad (5)$$

and that direct maximization of equation (4) with respect to α it is not possible. Substituting equation (5) into equation (4) gives

$$\log \mathcal{IG}(\mathbf{x}|\alpha) = -n(\alpha + 1) \overline{\log \mathbf{x}} - n \log \Gamma(\alpha) + n\alpha \log \alpha +$$

$$+n\alpha \log n - n\alpha \log \sum_{i=1}^n x_i^{-1} - \sum_{i=1}^n \frac{n\alpha}{x_i \sum_{j=1}^n x_j^{-1}} \quad (6)$$

Direct maximization of equation (6) with respect to α is (obviously) also not possible. Using the linear constrain

$$\alpha \log(\alpha) \geq (1 + \log \alpha_0)(\alpha - \alpha_0) + \alpha_0 \log(\alpha_0) \quad (7)$$

and substituting (7) into equation (6) provides a lower bound on the log-likelihood. Differentiating with respect to α and equaling to zero results in

$$\Psi(\alpha) = 1 + \log n\alpha_0 - \log \sum_{i=1}^n x_i^{-1} - \overline{\log \mathbf{x}} - \sum_{i=1}^n \frac{1}{x_i \sum_{j=1}^n x_j^{-1}},$$

where Ψ represents the *digamma function*. Noting that $\sum_{i=1}^n \frac{1}{x_i \sum_{j=1}^n x_j^{-1}} = 1$, we can simplify the expression to finally obtain

$$\alpha = \Psi^{-1} \left(\log n\alpha_0 - \log \sum_{i=1}^n x_i^{-1} - \overline{\log \mathbf{x}} \right). \quad (8)$$

Using the MM relationship for the shape parameter (equation 3, left side) to initialize α_0 in (8), and iteratively updating α_0 by α till convergence, we get $\hat{\alpha}$; we can then use equation (5) to get $\hat{\beta}$. Algorithm 2 summarizes the process:

Algorithm 2 ML for Inverse Gamma

Require: $\mathbf{x} = \{x_1, \dots, x_n\}, x_i > 0$
 $\mu = \bar{x} = \frac{1}{n} \sum_{i=1}^n x_i$
 $v = \frac{1}{n-1} \sum_{i=1}^n (x_i - \mu)^2$
 $\alpha = \frac{\mu^2}{v} + 2$
 $C = -\log \sum_{i=1}^n x_i^{-1} - \frac{1}{n} \sum_{i=1}^n \log x_i$
repeat
 $\alpha \leftarrow \Psi^{-1}(\log n\alpha + C)$
until convergence
 $\hat{\alpha} = \alpha$
 $\hat{\beta} = \frac{n\hat{\alpha}}{\sum_{i=1}^n x_i^{-1}}$
return $\hat{\alpha}, \hat{\beta}$

2.3 Bayesian Learning (BL)

Using Bayes rule to find the posterior probability of the Inverse Gamma parameters we have that

$$p(\theta|\mathbf{x}) = \frac{p(\mathbf{x}|\theta)p(\theta)}{p(\mathbf{x})}, \quad (9)$$

where $\theta = \{\alpha, \beta\}$ and $\mathbf{x} = \{x_1, \dots, x_n\}$ is some positive vector of observations. Since the denominator only depends on data the posterior is proportional to the likelihood multiplied by the prior

$$p(\theta|\mathbf{x}) \propto p(\mathbf{x}|\theta)p(\theta). \quad (10)$$

Obtaining analytical solutions for the parameters θ requires the use of conjugate priors [3, 6]. A prior is called conjugate with a likelihood function if the prior functional form remains unchanged after multiplication by the likelihood. Remember here that the likelihood of $\mathbf{x} = \{x_1, \dots, x_n\}$ under the Inverse Gamma distribution is

$$p(\mathbf{x}|\theta) = \mathcal{IG}(\mathbf{x}|\alpha, \beta) = \prod_{i=1}^n \frac{\beta^\alpha x_i^{-\alpha-1}}{\Gamma(\alpha)} \exp\left(\frac{-\beta}{x_i}\right). \quad (11)$$

Next, in subsection 2.3.1, we review the conjugate prior for the scale parameter and in subsection 2.3.2 we introduce the one missing in the literature, the conjugate prior for the shape parameter.

2.3.1 Scale parameter β

A well known conjugate prior for β , the scale parameter of the Inverse Gamma distribution, is a Gamma distribution parametrized using shape d and rate e [6],

$$p(\beta) = \mathcal{G}(\beta|d, e) = \frac{e^d \beta^{d-1}}{\Gamma(d)} \exp(-e\beta). \quad (12)$$

For completeness, in the remaining of this subsection we show that equation (12) is conjugate to the Inverse Gamma likelihood and provide the posterior expectation on β . Given the observations vector \mathbf{x} , we multiply the Inverse Gamma data likelihood (11) by the prior on scale (12) to get its posterior, $q(\beta)$

$$q(\beta) \propto \left(\prod_{i=1}^n \frac{\beta^\alpha x_i^{-\alpha-1}}{\Gamma(\alpha)} \exp\left(\frac{-\beta}{x_i}\right) \right) \frac{e^d \beta^{d-1}}{\Gamma(d)} \exp(-e\beta) \quad (13)$$

Keeping only β dependent terms

$$q(\beta) \propto e^d \beta^{d-1+n\alpha} \exp\left(-\beta\left(e + \sum_{i=1}^n x_i^{-1}\right)\right),$$

so the posterior is Gamma distributed $q(\beta) = \mathcal{G}(\beta|\hat{d}, \hat{e})$ with parameter values

$$\hat{d} = d + n\alpha, \quad \hat{e} = e + \sum_{i=1}^n x_i^{-1}. \quad (14)$$

Since β is Gamma distributed its posterior expectation is

$$\hat{\beta} = \frac{\hat{d}}{\hat{e}}. \quad (15)$$

2.3.2 Shape parameter α

Inspired by the unnormalized prior used for the shape parameter of the gamma distribution [6], we propose here an unnormalized prior for the shape parameter α of the inverse gamma distribution of the form

$$p(\alpha) \propto \frac{a^{-\alpha-1} \beta^{a\alpha}}{\Gamma(\alpha)^b}, \quad (16)$$

where β is the Inverse Gamma scale parameter and $\{a, b, c\} \in \mathcal{R}^+$ are hyper parameters. Given some observations \mathbf{x} , we multiply the associated likelihood under the Inverse Gamma distribution (11) by the proposed prior on shape (16) to obtain an expression for the posterior distribution $q(\alpha)$

$$q(\alpha) \propto \left(\prod_{i=1}^n \frac{\beta^\alpha x_i^{-\alpha-1}}{\Gamma(\alpha)} \exp\left(\frac{-\beta}{x_i}\right) \right) \frac{a^{-\alpha-1} \beta^{a\alpha}}{\Gamma(\alpha)^b}.$$

Keeping only α dependent terms we note that

$$q(\alpha) \propto \frac{\hat{a}^{-\alpha-1} \beta^{\alpha \hat{c}}}{\Gamma(\alpha)^{\hat{b}}} \quad (17)$$

with

$$\hat{a} = a \prod_{i=1}^n x_i, \quad \hat{b} = b + n, \quad \hat{c} = c + n. \quad (18)$$

This proves that equation (16) is a conjugate prior for the Inverse Gamma shape. Finding the posterior expectation of α , $\hat{\alpha}$, implies computing the expectation of $p(\alpha)$. Here we use the Laplace approximation to (16), which can be shown to be a Gaussian with mean

$$m = \Psi^{-1}\left(\frac{-\log a + c \log \beta}{b}\right),$$

and precision $b\Psi_1(m)$, where $\Psi_1(\alpha) = \frac{d\Psi(\alpha)}{d\alpha}$. Consequently we approximate the expected shape by

$$\hat{\alpha} \approx \Psi^{-1}\left(\frac{-\log \hat{a} + \hat{c} \log \beta}{\hat{b}}\right). \quad (19)$$

We note here that the expectation of the Laplace approximation to $q(\alpha)$ corresponds to the maximum a posteriori (MAP) estimate of $q(\alpha)$. The use of the Laplace approximation in this context then reduces to using a MAP estimation in place of the expected value. Note also that in order to compute the expectation (19) we need to estimate $\log \hat{a}$

$$\log \hat{a} = \log a + \sum_{i=1}^n \log x_i, \quad (20)$$

Algorithm 3 Bayesian learning for Inverse Gamma

Require: $\mathbf{x} = \{x_1, \dots, x_n\}, x_i > 0$ and $\{a, b, c, d, e\}$

$$\begin{aligned}\mu &= \frac{1}{n} \sum_{i=1}^n x_i \\ v &= \frac{1}{n-1} \sum_{i=1}^n (x_i - \mu)^2 \\ \alpha &= \frac{\mu^2}{v} + 2 \\ \hat{e} &= e + \sum_{i=1}^n x_i^{-1} \\ \log \hat{a} &= \log a + \sum_{i=1}^n \log x_i \\ \hat{b} &= b + n \\ \hat{c} &= c + n \\ C &= \log(\hat{e})\end{aligned}$$

repeat

$$\alpha \leftarrow \Psi^{-1}\left(\frac{-\log \hat{a} + \hat{c}(\log(d+n\alpha) - C)}{\hat{b}}\right)$$

until convergence

$$\begin{aligned}\hat{\alpha} &= \alpha \\ \hat{d} &= d + n\hat{\alpha} \\ \hat{\beta} &= \frac{\hat{d}}{\hat{e}} \\ \textbf{return } &\hat{\alpha}, \hat{\beta}\end{aligned}$$

and not longer require \hat{a} in equation (18). This fact has the advantage of avoiding numerical issues for large sample sizes. Further, substituting $\hat{\beta} = \frac{\hat{d}}{\hat{e}} = \frac{d+n\alpha}{e+\sum_{i=1}^n x_i^{-1}}$ into equation (19) we obtain an expression with no β dependence which is more compact for algorithmic use, namely

$$\hat{\alpha} \approx \Psi^{-1}\left(\frac{-\log \hat{a} + \hat{c}(\log(d+n\alpha) - \log(e + \sum_{i=1}^n x_i^{-1}))}{\hat{b}}\right). \quad (21)$$

Algorithm 3 summarizes the Bayesian approach for learning the Inverse Gamma parameters. First, the MM algorithm is used to initialize α (equation (3) left panel); \hat{e} , $\log \hat{a}$, \hat{b} and \hat{c} are computed through equations (14 right side), (20) and (18). Then equation (21) is iterated till convergence to obtain the expected $\hat{\alpha}$. Finally \hat{d} is computed using equation (14 left side) and $\hat{\beta}$ through (15).

2.4 KL-divergence

Let $p(x) = IG(x|\alpha, \beta)$ and $q(x) = IG(x|\hat{\alpha}, \hat{\beta})$ be two Inverse Gamma distributions with parameters $\{\alpha, \beta\}$ and $\{\hat{\alpha}, \hat{\beta}\}$ respectively. Then the KL-divergence between p and q is

$$KL[p||q] = (\alpha - \hat{\alpha})\Psi(\alpha) + \hat{\beta}\left(\frac{\alpha}{\beta}\right) - \alpha + \log \frac{\beta^{\hat{\alpha}+1}\Gamma(\hat{\alpha})}{\beta\hat{\beta}^{\hat{\alpha}}\Gamma(\alpha)}. \quad (22)$$

The proof is straight forward using the definition of KL divergence between the two distributions

$$KL[p||q] = \int_0^\infty p(x) \log \frac{p(x)}{q(x)} dx \quad (23)$$

and requires the use of

$$\int_0^\infty p(x)dx = 1, \quad (24)$$

$$\mathbb{E}_p[\log p(x)] = (1 + \alpha)\Psi(\alpha) - \alpha - \log(\beta\Gamma(\alpha)), \quad (25)$$

$$\mathbb{E}_p[\log x] = \log(\beta) - \Psi(\alpha), \quad (26)$$

$$\mathbb{E}_p[x^{-1}] = \frac{\alpha}{\beta}. \quad (27)$$

Equation (24) is a direct consequence of $p(x)$ being a pdf, and equations (25,26,27) can be easily derived from the definition of expectation of a function under a pdf

$$\mathbb{E}_p[f(x)] = \int_0^\infty p(x)f(x)dx. \quad (28)$$

3 Results

In section 3.1 we present examples demonstrating the methodology proposed to obtain the posterior expected shape in the Bayesian setting. Then in section 3.2 we present some theoretical and numerical results comparing the three different algorithms presented.

3.1 Visualizing the shape conjugate prior

In this section we provide numerical examples demonstrating the behavior of the posterior hyperparameter updates (equations 18,20) as well as that of the Laplace approximation (equation 19) used to obtain the expected shape $\hat{\alpha}$ in the Bayesian algorithm. We generate 1000 samples from an Inverse Gamma distribution with parameter values $\alpha = 10$ and $\beta = 25$. $\hat{\beta}$ is computed through equation (3) left panel followed by equations (14,15) where a flat prior was used, namely $d = e = 0.01$. For the shape prior hyper parameters we consider different values a, b, c , and $\hat{\alpha}$ is computed independently on each case through equations (18,20,19). In Figure 1, the top row shows the log-prior $\log p(\alpha|a, b, c, \hat{\beta})$ for the parameter values a, b, c indicated in the titles as a function of the shape value α represented in the x-axis. The bottom row shows the corresponding log-posteriors $\log p(\alpha|\hat{a}, \hat{b}, \hat{c}, \hat{\beta})$. In all cases the red dot represents the true shape value, $\alpha = 10$, and the green ones in the bottom row represents the posterior estimated value $\hat{\alpha}$. The log-posterior is much sharper around the correct value. The expectation we obtained for the posterior of α , $\hat{\alpha}$ marked as as green circle, is a very good approximation. Since the parameter value for the scale β was also estimated using Bayesian inference and its part of the prior and posterior on α , the figure indirectly confirms also the proper behaviour of the scale Bayesian estimation procedure.

These examples are representative of the general behaviour observed for a broad range of hyperparameter values $\{a, b, c\}$. Although this shows the weak dependence on the prior when estimating the posterior, further analyses to find flat priors would be of interest. In the next section we theoretically analyse the BL algorithm in relation to the ML to draw some light into this issue.

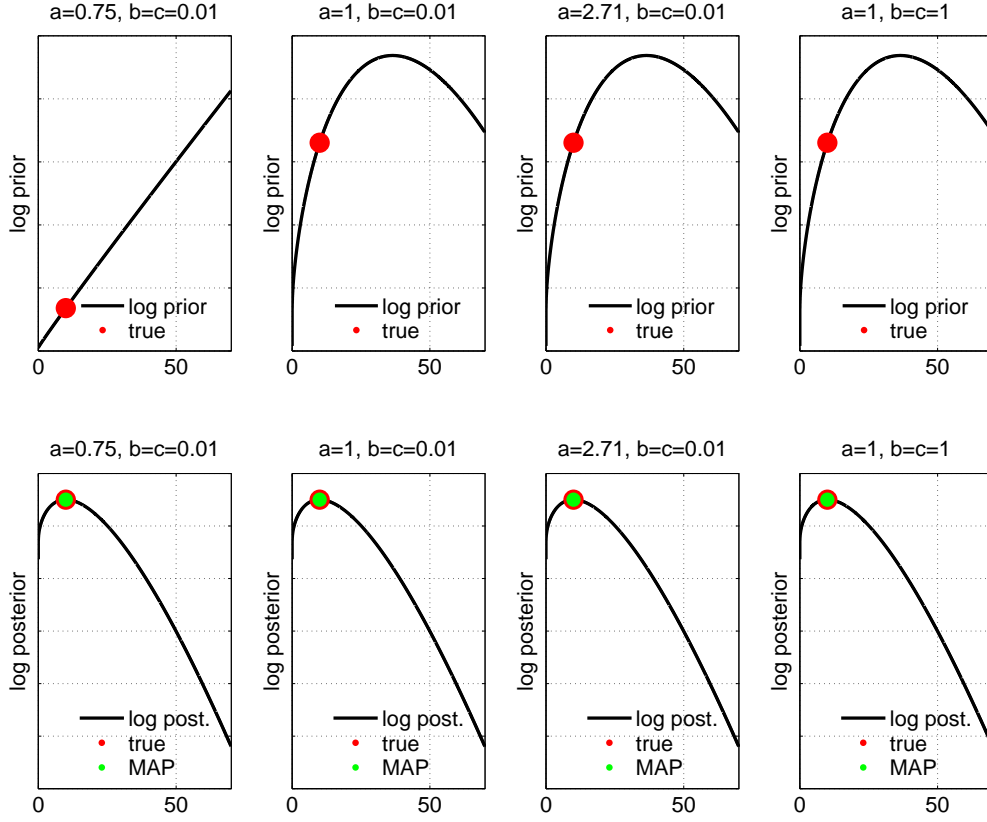


Figure 1: Top row shows the log-prior $\log p(\alpha|a, b, c, \beta)$ and the bottom row the log-posterior $\log p(\alpha|\hat{a}, \hat{b}, \hat{c}, \hat{\beta})$. The red dots mark the shape parameter α from which data was generated. The green dots represent the Bayesian posterior estimation.

3.2 Algorithms comparison

It is to note that ML and BL algorithms have notable similarities; first, note that the ML and the Bayesian scale estimators presented are

$$\hat{\beta}_{ML} = \frac{n\alpha}{\sum_{i=1}^n x_i^{-1}} \quad \hat{\beta}_{BL} = \frac{\hat{d}}{\hat{e}} = \frac{d + n\alpha}{e + \sum_{i=1}^n x_i^{-1}} \quad (29)$$

respectively. It is easy to observe that

$$\lim_{d=e \rightarrow 0} \hat{\beta}_{BL} \rightarrow \hat{\beta}_{ML}, \quad (30)$$

which means that the Bayesian scale estimator tends to the ML one in the limit of an infinite variance gamma prior over β . With respect to the shape parameter α , since initializing $b = c$ results in $\hat{b} = \hat{c}$, and taking again the same limit we can rewrite the Bayesian α update as

$$\lim_{\substack{d=e \rightarrow 0 \\ b=c}} \hat{\alpha}_{BL} \rightarrow \Psi^{-1} \left(\log n\alpha - \left(\log \sum_{i=1}^n x_i^{-1} \right) - \frac{\log a + \sum_{i=1}^n \log x_i}{\hat{b}} \right). \quad (31)$$

Comparing this to the ML α update

$$\hat{\alpha}_{ML} = \Psi^{-1} \left(\log n\alpha - \left(\log \sum_{i=1}^n x_i^{-1} \right) - \overline{\log \mathbf{x}} \right), \quad (32)$$

it is clear that both models perform an iterative update of the shape parameter dependent in the inverse of the gamma function of $\log n\alpha$ plus a data dependent constant which differs for ML and BL; they also have the same dependence on one of the data dependent terms, $\log \sum_{i=1}^n x_i^{-1}$, independently of the hyper parameter values used for the prior on α (under the assumption $b=c$). Further, since $\hat{b} = b + n$, in the extreme case of considering a very small hyper parameter value for b , we can simplify the Bayesian estimation update further, resulting in

$$\lim_{\substack{d=e \rightarrow 0 \\ b=c \rightarrow 0}} \hat{\alpha}_{BL} \rightarrow \Psi^{-1} \left(\log n\alpha - \left(\log \sum_{i=1}^n x_i^{-1} \right) - \overline{\log \mathbf{x}} - \frac{\log a}{n} \right). \quad (33)$$

Remembering that the posterior estimation for b and c are $\hat{b} = b + n$ and $\hat{c} = c + n$, this is a very interesting result that shows that when choosing little informative hyper parameter values for b and c , the Bayesian estimation involves a small sample bias correction term $\frac{-\log a}{n}$ which tends to 0 as the number of observed samples increases.

In the remainder of this section we perform a numerical comparison between the method of moments (MM), the maximum likelihood (ML) and the Bayesian approach (BL). For each simulation we generate varying amount of N samples from a Inverse Gamma distribution with fixed parameters α and β and we applied the three presented algorithms for estimating these. The parameter values α and β are initialized to different random positive numbers at each simulation. For each N we performed 500 different simulations. The ML and the BL algorithms are considered to converge when the relative α parameter change between two consecutive iterations is smaller than 10^{-6} . In this example the hyper parameter values are fixed to $a = b = c = 1$ and $d = e = 0.01$.

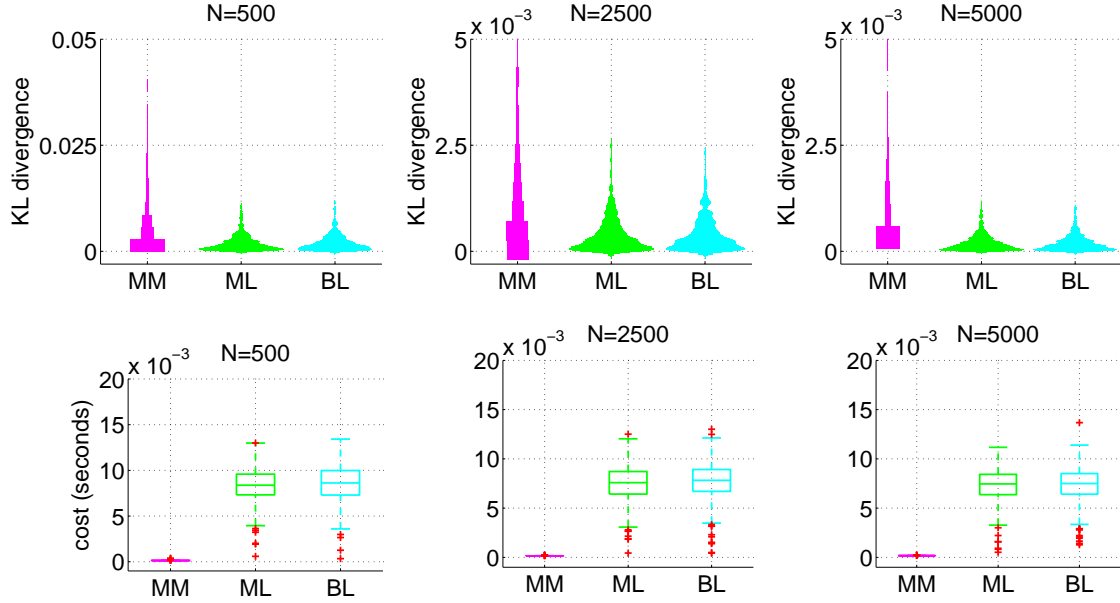


Figure 2: The top row shows violin plots of the KL divergences between the true and the estimated distributions for each of the 3 algorithms as indicated on the x-axis and for different number of observed samples (N) on each column. The different algorithms are also color coded for better visualization. The bottom row shows boxplots of the computational time required by the different algorithms expressed in seconds.

The top row of Figure 2 shows violin plots of the KL-divergences between the true and the estimated distributions for each of the 3 algorithms and for different number of observed samples (N) as indicated on each column. The method of moments (MM) shows larger deviations from the true distribution, while the ML and the BL algorithms provide very similar solutions. To assess statistical differences between the error obtained by the different algorithms we used a Wilcoxon rank test between each pair of models at each N independently and assess statistical significance at values $p < 0.01$. Independently of the number of samples, the MM algorithm is always significantly worse than the other two. The ML and the BL algorithm were not found to be significantly different. The bottom row shows boxplots of the computational costs in seconds; the mean, 25th and 75th percentile are presented on each box and the red crosses represent outliers of the estimated distributions. Obviously the ML and the BL approaches, as presented here, are more expensive than MM since they require iteration and in fact initialise with MM. The cost of both algorithms is equivalent which is not surprising given the theoretical comparison we performed previously. It is to note that in both cases the iterative process depends only on the inverse of the digamma function of a real number and there is no algorithmic cost N dependency in the loop. Interestingly, we also observed that a single iteration of the ML or the BL algorithms already suffices to significantly improve with respect to the MM.

On the basis of our analytic analyses we can conclude that small values for b and c are a reasonable choice, we further fixed these at values $b = c = 0.01$ and vary the values of a . We observed that the BL algorithm is no significantly different from the ML for a wide range of a values. As a reference, values of a in the range $[0.5, 5]$ were always optimal for simulations

analogous to the one presented in figure 2. Much higher or smaller values of a resulted in better solutions than MM but worse than ML; the difference with respect to ML was only observed at the smallest of the considered sample sizes, $N = 500$ samples and vanished for the higher sample sizes.

4 Discussion

We here presented three novel algorithms for the estimation of the parameters of a Inverse Gamma distribution and provide numerical evaluation of their estimation performance using synthetic data. The method of moments (MM) provides a closed form fast estimation; the maximum likelihood (ML) and the Bayesian approach (BL) use the method of moments as initialization and provide more accurate solutions, albeit at higher computational cost; these two algorithms significantly improve with respect to the method of moments already from the first iteration. We analytically studied the similarity between the ML and the BL algorithm and provided a range of hyper parameter values that provided solutions not deviating from the optimal ML estimation. The Bayesian Learning approach introduced in section 2.3 has important implications since it can be used inside more complex Bayesian inference tasks, such as fitting mixture models involving Inverse Gamma distributions within a (Variational) Bayesian framework to be used for example in the context of medical image segmentation [11]. Extending this beyond modelling one dimensional data, the presented methodology can also be included in multivariate models, e.g. for Bayesian ICA or Non-negative matrix factorizations.

References

- [1] H. Aksoy. Use of gamma distribution in hydrological analysis. *Journal of Engineering Environmental Science*, (24):419–228, 2000.
- [2] A. Balleri, A. Nehorai, and J. Wang. Maximum likelihood estimation for compound-gaussian clutter with inverse gamma texture. *Aerospace and Electronic Systems, IEEE Transactions on*, 43(2):775–779, April 2007.
- [3] C. M. Bishop. *Pattern Recognition and Machine Learning (Information Science and Statistics)*. Springer, 1 edition, 2007.
- [4] J. D. Cook. Inverse gamma distribution. Online: http://www.johndcook.com/inverse_gamma.pdf, Technical. Report, 2008.
- [5] F. Edgeworth. On the probable errors of frequency-constants. In *Journal of the Royal Statistical Society*, volume 71.
- [6] D. Fink. A compendium of conjugate priors, 1997.
- [7] A. Khalili, D. Potter, P. Yan, L. Li, J. Gray, T. Huang, and S. Lin. Gamma-normal-gamma mixture model for detecting differentially methylated loci in three breast cancer cell lines. *Cancer Inform*, 3:43–54, 2007.

- [8] D. J. C. MacKay. *Information Theory, Inference and Learning Algorithms*. Cambridge University Press, 2003.
- [9] T. P. Minka. Estimating a gamma distribution. *Microsoft Research*, 2002.
- [10] K. Pearson. Contributions to the Mathematical Theory of Evolution. Note on Reproductive Selection. *Proceedings of the Royal Society of London*, 59:300–305, 1895-1896.
- [11] M. Woolrich, T. Behrens, C. Beckmann, and S. Smith. Mixture models with adaptive spatial regularization for segmentation with an application to fmri data. *Medical Imaging, IEEE Transactions on*, 24(1):1–11, Jan 2005.
- [12] X. X. Shang and H. Song. Radar detection based on compound-gaussian model with inverse gamma texture. *IET Radar, Sonar and Navigation*, 5:315–321(6), March 2011.
- [13] S. Yue. A bivariate gamma distribution for use in multivariate flood frequency analysis. *Hydrological Processes*, 15(6):1033–1045, 2001.